Biotech SI

https://doi.org/10.17113/ftb.63.02.25.9020 original scientific paper

# A Comparative Study of Microbial Fuel Cells and Microbial Electrolysis Cells for Bioenergy Production from Palm Oil Mill Effluent

**Running Title: Microbial Innovations in Bioenergy from POME**

Abu Danish Aiman Bin Abu Sofian[1,2#], Vincent Lee[1#], Henry Marn Jhun Leong[1], Yeong Shenq Lee[1], Guan-Ting Pan[3] and Yi Jing Chan[1*]

[1]Department of Chemical and Environmental Engineering, University of Nottingham Malaysia, Broga Road, 43500, Semenyih, Selangor, Malaysia
[2]Department of Chemical Engineering, University of Manchester, Manchester, M13 9PL, United Kingdom
[3]College of Science, Health, Engineering & Education, Murdoch University, 90 South Street, Murdoch, WA 6150, Australia

Received: 28 December 2024
Accepted: 16 June 2025



## SUMMARY

*Research background.* The increasing environmental concerns due to fossil fuel consumption and industrial wastewater pollution necessitate sustainable solutions for bioenergy production and wastewater treatment. Palm Oil Mill Effluent (POME), a high-strength industrial wastewater, poses

*Corresponding author:
Prof. Dr. Yi Jing Chan
Phone: +6038924 8773
Email: yi-jing.chan@nottingham.edu.my

#These authors contributed equally

significant environmental challenges. Microbial Electrolysis Cells (MEC) and Microbial Fuel Cells (MFC) offer promising avenues for bioenergy recovery from such wastewaters.

*Experimental approach.* Dual-chamber H-type reactors equipped with proton exchange membranes were employed to separately assess MEC and MFC performance in bioenergy production from POME. Hydrogen generation and COD removal in MECs were evaluated at varying applied voltages and influent COD concentrations, while the impact of external resistance on power output and COD reduction was investigated in MFCs. Response Surface Methodology (RSM) was used to optimise these operational parameters for maximal bioenergy recovery and efficient wastewater treatment.

*Results and conclusions.* The findings revealed that hydrogen production and COD removal efficiency in MECs were maximised at low influent COD levels and low voltage supply. The MEC demonstrated effective hydrogen production and wastewater treatment, while the MFC achieved significant electricity generation and COD reduction. Field emission scanning electron microscopy confirmed the formation of biofilms on the electrodes, indicating active microbial communities involved in bioenergy generation. A trade-off between power density and COD removal efficiency in MFCs was observed, with medium resistance levels yielding maximum power output. The integration of MEC and MFC showed potential for treating high-strength industrial wastewater like POME, offering a greener and more energy-efficient approach.

*Novelty and scientific contribution.* This study demonstrates the potential feasibility of integrating MEC and MFC technologies for simultaneous bioenergy production and wastewater treatment from POME. It advances knowledge in biochemical engineering by optimising operational conditions for enhanced bioenergy recovery and highlights the role of microbial communities in bioelectrochemical systems. The findings provide a foundation for future research on sustainable bioenergy production and contribute to environmental sustainability efforts.

**Keywords:** microbial electrolysis cells; microbial fuel cells; hydrogen; palm oil mill effluent; proton exchange membrane; bioenergy

## INTRODUCTION

Malaysia is among the world's major palm oil exporters (*1,2*). However, the production of palm oil produces a huge amount of wastewater, namely POME (*3*). For every tonne of palm oil produced, approximately 5.0 to 7.5 tonnes of POME will be produced (*4*). POME is a highly polluting wastewater that contains a high amount of organic matter, where the COD concentrations range from 45,000 to

65,000 mg/L, the BOD concentration of 18,000 to 48,000 mg/L, and the oil and grease concentration of more than 2,000 mg/L (*5*). Its composition includes a range of readily fermentable carbohydrates and volatile fatty acids such as glucose, fructose, xylose, arabinose, acetate, and butyrate, which are favourable substrates for fermentative and electrogenic bacteria (*6*).

Anaerobic digestion is the most common way to treat POME due to its higher treatment effectiveness and high energy recovery (*7-9*). However, conventional AD faces several limitations in fully recovering the energy potential of POME. These include low and inconsistent methane yields due to the accumulation of inhibitory by-products, long hydraulic retention times, and sensitivity to fluctuations in POME composition, which can reduce process stability and energy recovery efficiency. To overcome these limitations, integrating bioelectrochemical systems such as MECs and MFCs has gained attention. However, given the distinct electrode architectures and electron transfer pathways of MEC and MFC (*10-12*), a dedicated focus on each system's performance in POME valorisation is necessary to fully exploit their respective potentials. These systems enhance energy conversion by utilising electroactive microbes to generate hydrogen (in MEC) or electricity (in MFC) directly from organic matter. MEC can achieve higher energy recovery by driving hydrogen production with minimal external energy input, while MFC enable simultaneous wastewater treatment and electricity generation. Moreover, both systems support additional resource recovery, including nutrients and biosolids, making them attractive for sustainable POME management. A comparison of MEC versus MFC under identical operating conditions will clarify the trade-offs between hydrogen and electricity yields, COD removal efficiency, and operational costs, thereby guiding the choice of the optimal technology for large-scale POME treatment. With over 400 palm oil mills operating in Malaysia, advancing such integrated systems is critical to addressing the industry's environmental and energy challenges (*13*).

The primary objective of this study is to evaluate the feasibility and potential of an integrated MEC-MFC system for the treatment of POME. The novelty of this research lies in the comparative analysis of individual dual-chamber H-type MEC and MFC for hydrogen and electricity production, respectively, while treating high-strength wastewater, with suggestions for future integration. The investigation focuses on the influence of applied voltage and influent COD concentration on hydrogen production and COD removal efficiency within the MEC, as well as the effect of resistance on MFC power density and COD removal. RSM is employed to optimise the MEC system by analysing the interactions between applied voltage and COD concentration. FESEM was used to confirm microbial presence within MEC and MFC systems, providing evidence of electroactive microbial activity. By addressing challenges related to internal resistance and effective POME treatment, this study aims

to contribute to the development of sustainable bioenergy technologies and promote resource recovery in the palm oil industry.

## MATERIALS AND METHODS

### *Wastewater collection*

POME and sludge samples were collected from a palm oil mill in Pahang, Malaysia and stored under anaerobic conditions at a refrigeration temperature of 4 °C prior to use. The collected POME exhibited a COD of 72,200 mg/L, while the sludge had a COD of 20,200 mg/L.

### *Reactor set-up*

A dual-chamber H-type reactor was used to operate both MEC and MFC. The reactor was composed of two identical reagent bottles, each with a plastic cap and a volume of 300 mL. The dual-chamber reactor was manufactured by Wente Experimental Ware (Changshu, China). The top of the reactor was constructed using rubber, allowing for the insertion of tubes and wires while maintaining an airtight condition. Each chamber has three main ports for circulation or extraction purposes.

Both anode and cathode chambers were separated by a Nafion membrane, which is a proton exchange membrane (PEM) (Nafion 117; Dupont; Wilmington, DE, USA) where it only allows free protons ($H^+$) to pass through (*14*). The Nafion membrane used had dimensions of 49 mm x 49 mm, resulting in a working area of 24.01 cm². The Nafion membrane was pre-treated by immersion in 5 *m*/*m* hydrogen peroxide at 80 °C for 1 hour, followed by deionised water for 30 minutes, then 5 *m*/*m* sulfuric acid at 80 °C for 1 hour, and finally rinsed again in deionised water for 30 minutes prior to use (*15*).

Graphite plate electrodes with dimensions of 70 mm (length) × 27 mm (width) × 2 mm (thickness) were used in both the anode and cathode chambers in MEC and MFC systems. Graphite was chosen for its excellent performance in open circuit voltage, current density, and power generation in microbial electrochemical systems (*16*). The total surface area of each rectangular electrode was 38.88 cm² after accounting for the glued wire area, the effective area was approximately 35 cm² (0.0035 m²), which was used in all performance calculations. The electrode spacing was maintained at approximately 8 cm to reduce internal resistance, consistent with the setup reported by Almatouq and Babatunde (*17*). The solution in the anode chamber was circulated using a magnetic stir bar, while the cathode chamber solution was circulated using a peristaltic pump (BT100J-1A; Longer Pump; Baoding, China). For MEC operation, a 1000 Ω resistor was connected between the cathode and the negative terminal of the DC power supply.

*Inoculation stage*

Biofilms were cultivated on the anodes of both MEC and MFC during the inoculation process, with some procedures common to both systems. Prior to inoculation, the pH of all solutions in both anode and cathode chambers was adjusted to neutral (pH 7) using either sodium hydroxide or hydrochloric acid. To establish anaerobic conditions in the anode chambers, pure nitrogen gas was purged for at least 20 minutes. In addition, all anolytes were supplemented with growth nutrients per litre of chamber volume: 0.984 g sodium acetate, 0.039 g potassium chloride, 0.15 g glucose, and 10 mL of tap water as a source of trace minerals. The inoculation process in both systems continued for a minimum of one month to allow the formation of stable and mature biofilms, which are essential for effective electron transfer and system performance.

In the MEC, the anolyte consisted of diluted POME mixed with deionised water at a ratio of 1:50, along with a 0.05 M phosphate buffer in a 1:1 ratio (*17*). The phosphate buffer used in the MEC anolyte was prepared using PBS (Phosphate Buffered Saline) with the following concentrations: 5.79 mM $NH_4Cl$, 17.77 mM $NaH_2PO_4 \bullet H_2O$, 32.23 mM $Na_2HPO_4$, and 1.74 mM KCl. To initiate biofilm formation, an external voltage of 0.9 V was applied to the system (*18*). Voltage was monitored continuously, and a decline toward 50 mV was used as an indicator of sufficient biofilm development, based on preliminary observations and supported by findings from Wang, Gao (*19*) who noted that voltage responses in MEC correlate with changes in biofilm conductance and activity. They reported that biofilm conductance increases with applied voltage and exhibits deviations from Ohm's law above 100 mV, indicating shifts in electron transfer mechanisms during biofilm growth. This suggests that sustained low voltages reflect electroactive and mature biofilms. Once this condition was reached, half of the anolyte was replaced with fresh phosphate buffer and substrate to replenish nutrients and maintain stable performance. Simultaneously, the external resistor was adjusted to 10 Ω to promote higher current flow and support continued biofilm activity.

In the MFC, the anolyte was composed of a mixture of 70 % diluted POME and 30 % sludge, and it was also in a 1:1 ratio with the phosphate buffer. The phosphate buffer used in the MFC anolyte had the same composition as described for the MEC. The anodes were connected to the positive pole of the power source, while the cathodes were connected to the negative pole via a 1 kΩ resistor.

*Experimental procedures*

Both MEC and MFC experiments were conducted in batch mode for three consecutive operating days and repeated twice weekly. Initial measurements of COD, pH, and conductivity were

taken from both chambers at the start of each run, and final measurements were recorded after the batch cycle.

The anode chamber solution was prepared by mixing 200 mL of diluted POME with 200 mL of 0.05 M phosphate buffer, resulting in a total volume of 400 mL. COD concentration was adjusted by varying the ratio of raw POME to deionised water in the dilution step. The use of diluted POME provided a natural source of microorganisms, including bacteria, essential for the bioelectrochemical processes (*20,21*). Despite the absence of added sludge, POME's organic matter and microbial load supported effective microbial activity. This setup was crucial for achieving the desired electrochemical reactions and demonstrated the practical application of using waste effluents directly in MFC/MEC systems. A volume of 300 mL of the prepared solution was used as the anode chamber solution, while the remaining 100 mL was used for various tests.

MEC operation

The preliminary experiment was conducted at different applied voltages (0.2 V, 0.7 V, and 1.2 V). Additionally, various COD levels (200 mg/L, 1000 mg/L, and 2000 mg/L) of the anode chamber solution were used. The schematic diagram of the MEC reactor is shown in Fig. S1a. The hydrogen gas produced in the cathode chamber was collected in an inverted 100 mL measuring cylinder submerged in water, and the volume was measured. Any gas generated in the anode chamber was collected in a gas sampling bag. The resistor connecting the cathode electrode to the power supply was changed to 10 Ω for this experiment. The hydrogen gas collected in the inverted measuring cylinder was transferred into a gas sampling bag after each experiment. At the end of each batch cycle, the reactors were exposed to air to inhibit methanogens and reduce the production of methane gas (*22*). This exposure was carefully controlled to minimise harm to the electroactive populations.

MFC operation

The experimental setup of the MFC is shown in Fig. S1b. The configuration of the MFC differed from that of the MEC, as the cathode chamber was aerated. The experiment was conducted using different resistor resistances (1 kΩ, 3.3 kΩ, 5.1 kΩ, 10 kΩ, 41 kΩ) to evaluate the MFC's performance under varying external loads. These resistances were selected to represent a range of typical loads used in MFC experiments, allowing for the analysis of how different resistances influence COD removal efficiency and voltage. This approach is consistent with established methods in MFC studies. For instance, Potrykus, León-Fernández (*23*) evaluated resistances from 0.12 kΩ to 3.3 kΩ, Li and Chen (*24*) evaluated 0.01kΩ to 10kΩ, and Kamau, Mbui (*25*) evaluated a higher range from 0.001 kΩ

to 33 kΩ. Furthermore, Kamau, Mbui (*25*) observed that the power generated increased from 0.00002 mW to 0.003131 mW when the external resistance was varied from 1 Ω to 33 kΩ on day 6. Evaluating a wide range of resistances is crucial to comprehensively understanding the MFC's performance characteristics. It helps to identify the optimal resistance for maximum power density, ensuring the system operates efficiently. Additionally, it provides insights into the operational limitations and potential areas for improvement in MFC design and operation. Therefore, a wide range of 1k Ω to 41 kΩ was evaluated in this study. The gas produced in the anode chamber was collected in a gas sampling bag via a hose connected through the top of the reactor. In this experimental setup, the cathode chamber was left open to allow the escape of air.

*Analytical methods and calculations*

Hydrogen produced in the MEC was collected in an inverted measuring cylinder immersed in water via a tube. The volume of hydrogen produced was determined by looking at the water level in the measuring cylinder, and the results were recorded every day. The hydrogen gas produced was kept in a gas sampling bag after the experiment. Gas chromatography (GC) (Clarus 580; PerkinElmer, Waltham, MA, USA) was employed to analyse the gas composition to confirm that hydrogen gas was produced.

The voltage across the resistor in both MEC and MFC was recorded every day using a digital multimeter. The current across the reactor was calculated using Ohm's law based on the voltage across the resistor, where $I=VR$. However, for MEC, the resistor will result in additional voltage loss in the system. Hence, the actual applied voltage, $E_{ap}$ to the reactor, was smaller than the voltage supplied by the power source, $E_{ps}$ (*22*). The actual applied voltage can be determined by using Eq. 1, where I is the current across the resistor and R is the resistance of the resistor.

$$E_{ap} = E_{ps} - IR \qquad /1/$$

Current density and power density were used to determine the performance of the MFC. The current density was calculated using the formula CD= I/A, where I=current and A=surface area of the anode electrode. The power density was calculated using the formula PD=P/A, where P = voltage x current, A= surface area of the anode electrode in $m^2$.

The COD levels of the anode solution in both MEC and MFC were measured before and after every experimental run to determine the COD removal efficiency using the Eq. 2.

$$\text{COD removal efficiency} = (COD_{initial} - COD_{final})/COD_{initial}*100 \qquad /2/$$

The COD levels of the solutions were measured using Hach High Range COD Digestion Vials at a range of 20-1500mg/L. A spectrophotometer (DR2800, Hach, United States) was used to detect

the COD levels of the solution in the vials. The conductivity of the anode and cathode solutions in both MEC and MFC was measured by using a conductivity meter (CON2700, Eutech, Netherlands) before and after every experimental run.

Coulombic efficiency (CE) was calculated using Eq. 3.

$$C_E = \frac{8Q}{F\,V_{an}\,\Delta COD} \qquad /3/$$

Where Q is the number of Coulombs, F is the Faraday constant, $V_{an}$ is the volume of the reactor in L, and ΔCOD is the amount of COD removed (*26*).

*Statistical analysis*

In the MEC experiment, RSM was employed to understand the impact of different parameters on the system's response and optimise its performance (*17*). Design Expert software by Stat-Ease Inc. was used for the design, analysis, and optimisation of this experiment. Two factors, namely COD concentration (A) and applied voltage (B), were considered, while the responses were hydrogen production rate and COD removal efficiency. Analysis of variance (ANOVA) was conducted to assess the regression of the fitted model, and the $R^2$ value was used to determine the goodness of fit of the model. The significance of the model was evaluated based on the Model F-value, and the significance of model terms was assessed using the P-value at a confidence level of 95 %. The software was used to identify the optimised operating conditions for the MEC system. To examine the effects of COD concentration and applied voltage on the hydrogen production rate and COD removal efficiency, a central composite design (CCD) was employed. CCD is chosen in this study as it is a widely used experimental design method that allows for the exploration of both linear and nonlinear relationships between variables (*11*). This approach allows for a systematic investigation of the relationship between the experimental factors and the desired responses, aiding in the identification of optimal conditions for improved bioenergy production and wastewater treatment efficiency in the MEC system.

## RESULTS AND DISCUSSION

*MEC*

According to the preliminary results presented in Table 1, the maximum cumulative hydrogen production observed in this experiment was 104.4 mL, corresponding to a hydrogen yield of 3.135 $m^3$ $H_2$/kg $COD_{removed}$. This value is higher than those reported by Marone, Ayala-Campos (*27*) (1.609 $m^3$ $H_2$/kg $COD_{removed}$) and Khongkliang, Jehlee (*28*) (0.236 $m^3$ $H_2$/kg $COD_{removed}$). The highest hydrogen production was observed at lower initial COD levels (<315 mg/L) and moderate applied voltages (0.199–0.652 V), whereas higher COD concentrations (790–1930 mg/L) and elevated voltages

(0.757–1.192 V) led to reduced yields. These findings suggest that the hydrogen production rate is influenced by both the initial COD level and the applied voltage.

Lower COD levels can mitigate substrate inhibition, promoting more effective microbial activity and bioelectrochemical processes, as high COD values can be detrimental to microorganisms (*29*). Additionally, using lower applied voltages can reduce competitive reduction reactions at the cathode, thereby improving hydrogen production efficiency. High applied voltages can induce oxidative stress, which may damage cells and diminish microbial growth and activity. This stress can restrict substrate oxidation, decrease proton ($H^+$) availability, and ultimately lower overall hydrogen production (*30*).

These results also highlight the importance of optimising operating parameters to achieve a balance between high COD removal efficiency, hydrogen production rate, and cost-effectiveness. While a voltage of 0.2 V resulted in significant hydrogen production in this study, this may be due to specific experimental conditions and might not apply to all MEC systems. According to Tan, Chong (*31*), the typical range of external voltages for MECs is 0.2 to 0.8 V to balance overpotential and internal resistance, which can affect hydrogen production efficiency. Logan, Call (*22*) further support this by noting that higher applied voltages increase the electrical energy input per amount of hydrogen produced (kWh/m³ $H_2$), emphasising the need to minimise energy losses while maintaining production rates. Additionally, Logan, Call (*22*) indicated that microbial electrolysis reactions generally start at applied voltages above 0.2 V, corresponding to an energy requirement of 0.43 kWh/m³ $H_2$ (at 100 % cathodic hydrogen recovery). Therefore, while these findings support the potential for lower voltage operation, further studies are necessary to generalise the results and optimise operating parameters for different MEC configurations to ensure cost-effective hydrogen production. This includes minimising electrical energy input to reduce overall operational costs and enhance the economic viability of MEC technology.

The highest CE achieved in this experiment was 97.69 %, which occurred at a COD level of 790 mg/L and a voltage of 1.104V. Some CE values were unavailable due to the unchanged COD level after the experiment. The CE values ranged from 0.91 % to 97.69 %, aligning with the findings of Hari, Venkidusamy (*32*), where CE ranges from 50 % to 90 %, depending on operational conditions and substrate type. It was observed that CE was influenced by the current across the reactor and the amount of COD removed. Specifically, CE increased as the current across the reactor increased, while higher COD removal corresponded with a decrease in CE. The microbial community can efficiently utilize the available substrate at lower COD levels, leading to higher CE. In contrast, at higher COD levels, substrate inhibition may reduce microbial efficiency, lowering CE. Similarly, higher voltages can enhance microbial electroactivity, but they may also increase competition for electrons

and trigger side reactions, leading to lower CE. These factors contribute to the observed variability in CE, highlighting the complexity of microbial electrochemical processes and emphasising the need for careful optimisation of operational parameters to achieve consistent and high CE in MEC systems.

Furthermore, a direct correlation was observed between the COD level in the anode chamber and the pH difference between the anode and cathode chambers (Table 1). Higher COD levels resulted in greater pH disparities between the two chambers, leading to increased potential loss (*17*). To address this issue, a phosphate buffer solution was employed in the experiment to maintain a balanced pH within the system. For each 300 mL chamber, approximately 50-100 mL of phosphate buffer was employed based on preliminary tests to stabilise the pH. However, it is important to note that the use of phosphate buffer solution in large-scale MEC applications poses a significant challenge due to its high cost and the potential environmental impact associated with the disposal of large volumes of used phosphate buffer solution (*33*). These considerations necessitate further exploration and development of alternative pH control strategies for MEC scaling-up efforts.

To further investigate the effects of the independent variables (COD concentration and applied voltage) on hydrogen production rate and COD removal efficiency, 9 experimental conditions based on the Central Composite Design (CCD) were conducted in the laboratory. Based on the preliminary results, the ranges of influent COD concentration (mg/L) and voltage were determined (Table 1). According to the CCD, the observed experimental results regarding hydrogen production in the MEC are provided in Table 2.

*MEC cumulative hydrogen production*

The ANOVA results (Table S1) indicated a significant 2FI (Two Factor Interaction) model, suggesting that both influent COD concentration (A) and voltage supply (B), as well as their interaction (AB), influenced hydrogen production rate. The high $R^2$ value of 0.9918 and adjusted $R^2$ value of 0.9868 indicate that the model is well-fitted to the data, with a strong degree of fitness. This implies that the model can explain a significant portion of the variability in the hydrogen production rate.

The response surface plot, as shown in Fig. 1, provides a visual representation of the relationship between the two factors and cumulative hydrogen production. It illustrates the influence of the factors on the response variable and can be used to identify optimal operating conditions for maximising hydrogen production. All the model terms were statistically significant, as indicated by the low P-values (less than 0.1) (Table S1). This suggests that each factor and its interactions significantly impact cumulative hydrogen production. The model F-value of 201 indicates that the model was significant, with a 0.01 % chance that a large F-value could occur due to noise. The following model

(Eq. 4) explains the hydrogen production rate, where A is influent COD concentration, and B is the voltage supply:

Hydrogen production rate = 8.96 – 29.17 × (COD concentration) – 19.01 × (Voltage supply) – 23.67 × (COD concentration × Voltage supply) /4/

A negative term in Eq. 4 indicates an inverse relationship between the manipulated variables (influent COD level and voltage supply) and the response variable (hydrogen production rate). This shows that both higher COD levels and higher voltages reduce hydrogen production. The significant interaction term between A and B (−23.67AB) suggests a synergistic negative impact, meaning that when both A and B are present, the reduction in hydrogen production is greater than the sum of their individual effects. Therefore, optimising both parameters simultaneously to maximise hydrogen production is essential.

This finding is consistent with the 3D surface graph presented in Fig. 1, where hydrogen production increased at low COD levels and moderate voltage. This may be attributed to more favourable microbial conditions under low organic loading, where excessive substrate or voltage could disrupt microbial balance or induce inhibitory effects (*24*). These insights support the need for careful tuning of both variables to maintain microbial performance and maximise hydrogen yield.

*MEC COD removal performance*

The ANOVA results for COD removal efficiency are presented in Table S1. Similar to the hydrogen production rate, a high $R^2$ value of 0.9639 and an adjusted $R^2$ value of 0.9518 are obtained, which indicates a good degree of fitness for the model. This suggests that the model can accurately explain the variability in COD removal efficiency. The significance of the model is further supported by the model F-value of 80.05, which indicates a 0.01 % chance that such a large F-value could occur due to noise.

COD removal efficiency (%) = 16.89 – 26.07(COD concentration) – 8.02(Voltage supply) /5/

The linear model presented in Eq. 5 describes the relationship between COD removal efficiency and the influencing factors. This model indicates that lower COD concentrations and voltage levels promote better organic degradation. This is because high COD levels may exceed microbial degradation capacity, while elevated voltages could negatively impact microbial viability (*22*). The

negative coefficients in the equation indicate an inverse effect between the manipulated variables (influent COD level and voltage supply) and the response variable (COD removal efficiency). This suggests that as the influent COD level and voltage supply decrease, the COD removal efficiency increases.

This finding is consistent with the observed relationship in the hydrogen production rate (Fig. 1). The 3D surface graph in Fig. 2 illustrates this relationship, showing that higher voltage supply leads to lower COD removal efficiency. This is possibly attributed to the potential negative effects of high voltage on microorganisms, which can hinder their ability to effectively degrade organic matter (*34*).

Furthermore, the COD removal efficiency decreases as the solution's COD level increases. This can be attributed to the limited time available for the microorganisms to degrade higher concentrations of organic matter, resulting in lower efficiency. Therefore, lower COD levels in the solution are associated with higher COD removal efficiency. To achieve higher COD removal efficiency at higher COD levels, longer retention times may be required to provide sufficient opportunity for complete degradation.

In summary, these findings highlight the critical role of controlling the influent COD level and voltage supply to achieve optimal performance in MEC. By lowering the influent COD level and selecting suitable voltage levels, significant improvements can be achieved in both COD removal efficiency and hydrogen production rate. This not only enhances the overall system efficiency but also reduces energy consumption. Building upon these results, further optimisation strategies were implemented, which will be discussed in the following section.

*MEC parameter optimisation*

The empirical model represented by Eqs. 4 and 5 was evaluated using the Design-Expert software to determine the optimal conditions for maximising hydrogen production and COD removal efficiency. Table S2 presents the results of the optimisation process, where the initial COD level and voltage supply were adjusted within the specified operating range to achieve the maximum hydrogen production rate and COD removal efficiency. The optimal operating condition was identified at a COD level of 150 mg/L and a voltage supply of 0.338 V, with a high desirability value of 0.966 (Table S2). The findings suggest that maximising the hydrogen production rate and COD removal efficiency can be achieved by employing low influent COD levels and a low voltage supply. This is consistent with previous reports stating that hydrogen production is achievable at applied voltages as low as 0.2 V, although values below 0.3 V may lead to low hydrogen production rates and unstable system

performance (*35*). Operating at lower voltages offers practical advantages, including reduced energy consumption and lower operational costs. Furthermore, minimising power input aligns with sustainability goals by reducing carbon emissions associated with MEC operation.

*MEC anode biofilm characterisation*

Field emission scanning electron microscopy was employed to examine the biofilm on the anode electrode, revealing bacterial presence at a magnification of 20,000x as shown in Fig. 3a. While FESEM is a valuable tool for visualising biofilm structure and bacterial colonisation, it does not provide definitive species identification. For example, Mejía-López, Verea (*36*) used FESEM in their MEC studies to show that bacteria preferentially attached to particles on the electrode surface, with populations exhibiting uniform morphology and distribution.

The observation of bacterial biofilms supports the hypothesis that microbial processes contribute to hydrogen production. Previous studies by Wang, Liu (*37*), Liu, Wang (*38*), and Logan, Call (*22*) have reported the presence of *Pseudomonas* spp. and *Shewanella* spp. in similar MEC systems. Liu, Wang (*38*) specifically noted that "rod-like" bacteria are likely the functional strains with electrochemical activity. This was supported by single-strand conformation polymorphism (SSCP) analysis, which identified *Pseudomonas* sp. and *Shewanella* sp. as dominant during the hydrogen-production stage. The rod-shaped bacteria observed in this study (Fig. 3a-b) suggest that similar species could be present. This aligns with established knowledge of microbial communities in MECs, despite the lack of additional molecular identification techniques.

Acknowledging the limitations of FESEM, further research involving molecular methods, such as PCR or 16S rRNA sequencing, is necessary for precise species identification. However, FESEM effectively demonstrates microbial biofilm formation and supports the role of microbial activity in hydrogen production. This preliminary observation provides a foundation for subsequent studies aimed at characterising specific bacterial species and their contributions to the MEC process.

*MFC*

The MFC experiment was conducted using different resistor resistances, and the corresponding results are presented in Table 3. It is important to note that the composition of the anode solution in the MFC differs from that of an MEC. In the MFC, the anode solution is prepared by combining raw sludge and diluted POME. To ensure consistency, the quantities of raw sludge, raw POME, and deionised water were kept constant throughout the experiment. The focus of this experiment was solely on manipulating the resistor by using different resistances. By maintaining

consistency in the anode solution and varying the resistor resistances, the study aimed to explore the influence of this parameter on the performance of the MFC.

*MFC Power and current density profiles*

The power density of a system is often used to compare its power output. The power output of a system is determined by the projected area of the anode electrode, where biological reactions occur (*39*). The maximum power density recorded was 2.096 mW/m$^2$ at a current density of 10.43 mA/m$^2$ and a resistance of 5100 Ω (Batch 3, Table 3). It is observed that power density increases as the current density in the MFC increases. While relatively low, this value is comparable to those reported by Chonde (*40*), which is 2.87 kW/m$^3$, and is slightly lower than the values reported by Zain, Roslani (*41*), who achieved a maximum power density of 9.053 mW/cm$^2$ using activated sludge. Similarly, Ghangrekar and Shinde (*42*) reported a power density of 6.73 mW/m$^2$, and Fischer, Sugnaux (*43*) achieved 16.2 mW/m$^2$.

Previous MFC studies reviewed by Tan, Chong (*31*) and Obileke, Onyeaka (*44*) have achieved higher power densities, ranging from 78 to 460 mW/m$^2$. These higher values can be attributed to differences in electrode materials, operational conditions (temperature, pH), pure culture or mixed culture inoculum, proton exchange system (PES), and design and configuration of MFC reactors (*44*). For example, Daud, Daud (*45*) fabricated a novel porous clay earthenware (NCE) as a low-cost separator to replace the high-cost PEM (Nafion 117). Their experiments revealed the highest power and current densities recorded were 2250 ± 21 mW/m$^2$ and 6.0 A/m$^2$, respectively, using the NCE low separator and 30 vol % starch powder content under batch mode operation.

The lower power densities obtained in this study are primarily due to non-optimised conditions and less conductive electrode materials. The methodology focused on exploring the basic principles of MFC operation and integration with MEC rather than optimising power output. Future research will aim to improve the performance by optimising conditions and exploring advanced materials and reactor designs.

The polarisation curve, also known as the voltage-current (V-I) curve (Fig. 4), is essential for understanding the operation of MFC, as it represents the voltage at different current densities (*39*). This curve is divided into three distinct regions: activation losses, ohmic losses, and concentration losses (*22*). The first region, characterised by a steep decrease in voltage at zero current, reflects activation losses. These losses are due to the high energy barrier needed to initiate oxidation or reduction reactions, where electrons are transferred from bacteria to the anode surface (*22*). To

minimise activation losses and enhance electron transfer efficiency, strategies such as increasing the anode's surface area and using materials with higher catalytic activity can be employed.

The second region of the polarisation curve corresponds to ohmic losses, where the voltage drop becomes more constant and shows a linear relationship with the current. These losses arise from the resistance of the solution and the membrane. In this region, the slope of the polarisation curve indicates the internal resistance of the MFC, with a lower slope being more desirable as it signifies reduced resistance and higher efficiency. Ohmic losses can be mitigated by minimising the distance between electrodes and selecting membranes with lower resistivity and higher ionic conductivity (*22*).

The final region of the curve highlights concentration losses, which occur at higher currents and are indicated by a sharp voltage decline. These losses result from mass transfer limitations, where the rate of reaction is insufficient to maintain the flux of reactants to the electrode or the flux of products away from the electrode (*22*). To address concentration losses, potential strategies include optimizing electrode design for improved mass transfer, adjusting flow rates within the MFC, and employing catalysts to accelerate reaction kinetics (*46*).

The internal resistance of the MFC, approximately 5.3 kΩ, was determined from the slope of the V-I curve (Fig. 4). This internal resistance can be reduced by minimising the electrode spacing and selecting a membrane with low resistivity. The power density curve, represented by the P-I curve in Fig. 4, provides further insights into MFC performance. The P-I curve shows that power density increases with increasing current density. This trend suggests that the system's power output improves as current density increases, likely due to more efficient electron transfer and energy conversion at higher currents. Understanding and analysing these curves enables the development of targeted strategies to enhance MFC efficiency, ultimately improving performance in practical applications.

The power generation of the MFC is also depicted in Fig. S2. This figure shows how the power output changes over time during the operation of the MFC. It initiates with a very low power generation due to the initiation of oxidation or reduction reactions. It peaks on the second and third day of operation and gradually decreases towards the final day. This decline in power generation can be attributed to the limited reaction rate. The coulombic efficiency of the MFC ranges from 0.036 % to 0.076 %, with higher efficiencies achieved at increased current across the reactor.

*MFC COD removal vs. applied voltage*

Fig. 5 shows a clear relationship between resistance and voltage in the MFC system. As resistance increases, voltage also increases. This finding aligns with the proportionality between

resistance and voltage described by the equation V = IR. Similarly, the COD removal efficiency shows an increasing trend up to a peak value at around 10,000 ohms, after which it decreases. This finding aligns with the results reported by Kloch and Toczyłowska-Mamińska (*47*), which showed a substantial increase of around 30 % in COD removal efficiency when the external resistance was raised from 100 ohms to 1000 ohms. These findings highlight the critical role of external resistance as a key parameter in MFC systems. The observed increase in COD removal efficiency with higher resistance suggests that elevated resistance values can stimulate improved performance in terms of organic matter degradation. However, it is important to note that beyond a certain resistance threshold, the efficiency begins to decline. This indicates the existence of an optimal resistance range that balances microbial activity and bioelectrochemical processes involved in COD removal. Therefore, the selection of the external resistance is crucial for the long-term operation of MFCs, as it directly impacts the microbial community responsible for bioelectricity generation (*48*).

Besides, this study found that medium resistance values (5100 Ω) resulted in maximum power density, while high resistance values (10000 Ω) led to high COD removal efficiency. This suggests a trade-off between power density and COD removal efficiency in the MFC system. This trade-off is driven by the dynamics of substrate availability, electron flow, and microbial activity. At higher resistance values, the slower electron flow allows for more complete oxidation of organic matter, enhancing COD removal but reducing power density. Conversely, at lower resistance values, faster electron flow favours higher power density but can result in incomplete COD removal. Optimal performance in terms of power density and COD removal efficiency may require finding a balance between resistance values that maximize power output and those that enhance organic matter degradation. Approaches such as dynamic resistance adjustment, optimizing microbial consortia, and improving electrode materials could help to balance these parameters. Further investigation is needed to explore this relationship and identify the optimal resistance range that balances power density and COD removal efficiency.

*MFC pH dynamics*

According to the results presented in Table 3, there was a noticeable increase in the final cathode pH compared to the initial pH value of 7. The final pH of the cathode ranged from 7.41 to 7.51. This observed increase in pH in the cathode chamber can be attributed to the cathode reaction, during which protons are consumed and hydroxyl anions are released into the solution (*26*). The final pH values for the anode ranged from 7.13 to 7.41. These changes in pH provide valuable insights into the electrochemical processes taking place within the MFC system. Maintaining proper control

and regulation of pH levels in the cathode chamber is crucial for optimising the performance of the MFC. Fluctuations in pH can have significant implications for the overall efficiency and stability of the system. Further investigation and optimisation strategies can be explored to mitigate any potential negative effects associated with pH changes and maximise the performance of the MFC.

*MFC anode biofilm characterisation*

FESEM was conducted to examine the morphology and distribution of microorganisms on the anode electrode in the MFC, aiming to draw comparisons to those observed in the MEC. FESEM provides detailed surface images that allow for the visualisation of microbial structures at the nanoscale (*49*). This analysis revealed the presence of rod-shaped bacteria on the anode surfaces in both MFC (Fig. 3c-d) and MEC (Fig. 3a-b) systems, consistent with observations reported by Liu, Wang (*38*). This finding aligns with previous studies indicating that *Pseudomonas aeruginosa* can generate electricity in MFCs through the production of organic compounds such as phenazine pyocyanin, which facilitate electron transfer from the bacterium to the anode (*50*). Based on Fig. 3c-d, the presence of rod-shaped bacteria suggests that *Pseudomonas aeruginosa* may be among the microorganisms on the MFC electrode surface. Although FESEM alone does not definitively identify bacterial species, these findings provide valuable insights into the potential role of similar microbial processes in both MFCs and MECs. This assumption presents opportunities for future investigations into the utilisation of *Pseudomonas aeruginosa* and related *Pseudomonas* species in MFCs to enhance bioelectrochemical energy generation. Molecular methods such as 16S rRNA sequencing should be employed in future studies to confirm bacterial species and assess the potential benefits and challenges of harnessing these bacteria in both MFC and MEC systems. Additionally, further research is needed to elucidate the specific mechanisms involved and to evaluate the potential benefits and challenges associated with these bacteria in bioelectrochemical systems.

*Future perspectives: Integration of MFC and MEC*

Although the integration of MFC-generated electricity to power the MECs was not implemented in this study, it is proposed as a future research direction. The MEC experiment revealed that a voltage of 0.3 V resulted in the highest hydrogen gas production and COD removal efficiency. By utilising an MFC with a 5100Ω resistor, this voltage range could potentially be provided to power the MEC, eliminating the need for an external voltage supply and reducing costs. Exploring the integration of MFC-generated electricity to power MECs for hydrogen gas production may offer improved results, considering the higher profit potential of hydrogen gas compared to electricity

generation. Such integration of MEC and MFC technologies could present a greener and more environmentally friendly approach to power generation and wastewater treatment. When compared to other integrated systems, such as those that combine anaerobic digestion with microbial fuel cells, MEC-MFC integration uniquely combines electricity generation with hydrogen production, though similar systems also encounter challenges related to operational management and optimisation.

Future perspectives on the integration of MEC and MFC technologies involve several key considerations. Potential configurations include directly coupling MFC to power MEC, using MFC-generated electricity to drive MEC processes, and employing reactor effluent from one system as influent to the other to optimise performance. Practical considerations for implementation include ensuring reactor material compatibility, managing operational parameters such as pH and temperature, and scaling up from laboratory to industrial scales. The integration is expected to reduce external energy requirements and enhance overall system efficiency. However, challenges such as balancing power density with COD removal efficiency and managing increased system complexity need to be addressed.

In terms of scalability, attention must be given to material durability, particularly for electrodes and membranes, to withstand long-term operational stresses. Additionally, maintaining stable microbial communities over extended periods is crucial for sustained performance. Furthermore, the increased complexity of integrated systems may necessitate advanced monitoring and control strategies to ensure consistent operation at larger scales. The development of submergible and stackable MFCs or electrode modules, as highlighted by Tan, Chong (*31*), could also play a crucial role in enhancing scalability and operational flexibility. Moreover, integrating membrane-less systems or low-cost membranes may further reduce costs and enhance the feasibility of large-scale deployment (*31*).

In terms of economic considerations, both MEC and MFC have similar capital costs due to their similar architecture in this experiment. Moreover, they are environmentally friendly and safe, as they do not require toxic chemicals to facilitate reactions. Additionally, these technologies are not labour-intensive and do not require large operational areas. However, it is important to note that the cycle time for both processes is around 3 to 4 days to produce sufficient bioenergy. This relatively long cycle time may impact the efficiency and scalability of these systems, potentially leading to increased operational costs and slower throughput. Efficient integration of these technologies into existing wastewater treatment infrastructure would benefit from addressing these cycle time challenges to optimise performance and cost-effectiveness.

In summary, integrating MEC and MFC technologies is a highly feasible concept for sustainable bioenergy production and wastewater treatment. The experimental results provide

valuable insights into the operational parameters, efficiency, and potential benefits of this integrated approach. Further research and optimisation efforts are crucial to enhance process efficiency, reduce cycle times, and address key factors for scalability and long-term stability. Investigating strategies for integrating MEC and MFC technologies into existing wastewater treatment infrastructure will be essential for their practical application. Additionally, future research should include additional parameters such as volatile fatty acids (VFAs), total nitrogen, and other soluble organics, alongside pH and COD, to offer a more comprehensive understanding of substrate impacts.

## CONCLUSION

This study concludes that dual-chamber reactors, separated by a proton exchange membrane, are effective in hydrogen production in MEC and electricity generation in MFC for POME treatment and bioenergy generation. The MECs demonstrated successful hydrogen gas production with a maximum yield of 3.135 $m^3$ $H_2$/kg COD removed and 48.7 % COD removal at an influent COD level of 150 mg/L and a voltage supply of 0.338 V. In addition, the MFCs exhibited electricity generation, achieving a maximum power density of 2.10 mW/$m^2$, a voltage of 0.20 V, and a current density of 10.43 mA/$m^2$ at a resistance of 5100 Ω. These findings highlight that low influent COD and low applied voltage enhance hydrogen production by maintaining microbial activity and reducing inhibitory effects. Furthermore, the MFC operating with a 5100 Ω resistor was able to generate sufficient voltage (0.3 V) to power the MEC without external energy input, demonstrating the potential for energy self-sufficiency and improving the sustainability and cost-effectiveness of the system. However, despite these promising outcomes, several challenges remain for scaling up. The optimum conditions observed at low COD levels may not directly translate to industrial effluents, which typically have higher and more variable COD concentrations that could affect system stability and performance. Long-term biofilm stability and microbial community control under fluctuating conditions remain critical concerns. Compared to previous research, this work introduces a novel integration of MFC and MEC systems using real POME as substrate, offering a low-carbon pathway for waste-to-energy applications in the palm oil industry. Insights gained provide a foundation for scale-up, which will require addressing operational issues like mass transfer limitations, electrode fouling, and energy balance. Future work should focus on system integration optimisation, biofilm robustness, and microbial dynamics to improve resilience and energy recovery. Investigating additional parameters such as volatile fatty acids, nitrogen, and other organics will enhance understanding of substrate effects. Efforts to integrate these technologies into existing treatment infrastructure will be vital for practical application.

## ACKNOWLEDEGMENT

The authors acknowledge the support provided by the University of Nottingham Malaysia in this research project. A.D.A. Bin Abu Sofian thanks the University of Manchester for awarding him the Dean's Doctoral Award.

## FUNDING

The authors acknowledge the financial support for equipment, materials and testing provided by the University of Nottingham Malaysia in this research project.

## CONFLICT OF INTEREST

The authors declare no conflict of interest.

## SUPPLEMENTARY MATERIAL

Supplementary materials are available at: www.ftb.com.hr.

## AUTHORS' CONTRIBUTION

A.D.A. Bin Abu Sofian and V. Lee contributed equally as co-first authors. They conceived and designed the study, collected the data, performed the initial analysis, drafted the manuscript, and critically revised it for important intellectual content. H.M.J. Leong and Y.S. Lee contributed to data interpretation, critically reviewed the manuscript, and approved the final version for publication. G.-T. Pan supported the study's design, performed advanced data analyses, and critically evaluated the manuscript. Y.J. Chan, as the corresponding author, coordinated the overall research activities, supervised data analysis, critically reviewed the manuscript for important content, and approved the final version for publication. All authors read and approved the final manuscript.

## ORCID ID

A.B.D. Bin Abu Sofian https://orcid.org/0009-0006-2360-0449
Y.S Lee https://orcid.org/0009-0005-6853-7212
G. T. Pan https://orcid.org/0000-0003-3565-2802
Y.J. Chan https://orcid.org/0000-0003-2123-2356

## REFERENCES

*1*.Chan YJ, Chong RJW, Chong MF, Ng DKS, Lim LK. Performance and Stability of Pre-commercialized Integrated Anaerobic–Aerobic Bioreactor (IAAB) for the Treatment of Palm Oil Mill

Effluent (POME). Sustainable Technologies for the Oil Palm Industry: Latest Advances and Case Studies: Springer; 2022. p. 301-23. https://doi.org/10.1007/978-981-19-4847-3_12.

*2*.Syahid LN, Luo X, Zhao R, Lee JSH. Climate drives variation in remotely sensed palm oil yield in Indonesia and Malaysia. Environ Res Lett. 2025;20(4):044016. 10.1088/1748-9326/adbfac

*3*.Bhatia SK, Patel AK, Ravindran B, Yang Y-H. Renewable bioenergy from palm oil mill effluent (POME): A sustainable solution for net-zero emissions in palm oil production. J of Water Process Eng. 2025;70:107136. https://doi.org/10.1016/j.jwpe.2025.107136

*4*.Mamimin C, Singkhala A, Kongjan P, Suraraksa B, Prasertsan P, Imai T, et al. Two-stage thermophilic fermentation and mesophilic methanogen process for biohythane production from palm oil mill effluent. Int J Hydrogen Energy. 2015;40(19):6319-28. https://doi.org/10.1016/j.ijhydene.2015.03.068.

*5*.Tan VWG, Chan YJ, Arumugasamy SK, Lim JW. Optimizing biogas production from palm oil mill effluent utilizing integrated machine learning and response surface methodology framework. J Clean Prod. 2023;414:137575. https://doi.org/10.1016/j.jclepro.2023.137575.

*6*.Taifor AF, Zakaria MR, Mohd Yusoff MZ, Toshinari M, Hassan MA, Shirai Y. Elucidating substrate utilization in biohydrogen production from palm oil mill effluent by Escherichia coli. Int J Hydrogen Energy. 2017;42(9):5812-9. https://doi.org/10.1016/j.ijhydene.2016.11.188

*7*.Choong YY, Chou KW, Norli I. Strategies for improving biogas production of palm oil mill effluent (POME) anaerobic digestion: A critical review. Renew Sust Energ Rev. 2018;82:2993-3006. https://doi.org/10.1016/j.rser.2017.10.036.

*8*.A. Shukla K, Bin Abu Sofian ADA, Singh A, Chen WH, Show PL, Chan YJ. Food waste management and sustainable waste to energy: Current efforts, anaerobic digestion, incinerator and hydrothermal carbonization with a focus in Malaysia. J Clean Prod. 2024;448:141457. https://doi.org/10.1016/j.jclepro.2024.141457

*9*.Singh A, Bin Abu Sofian ADA, Chan YJ, Chakrabarty A, Selvarajoo A, Abakr YA, et al. Hydrothermal carbonization: Sustainable pathways for waste-to-energy conversion and biocoal production. GCB Bioenergy. 2024;16(6):e13150. https://doi.org/10.1111/gcbb.13150

*10*.Nor NAM, Tanaka F, Yoshida N, Jaafar J, Zailani MZ, Ahmad SNA. Preliminary evaluation of electricity recovery from palm oil mill effluent by anion exchange microbial fuel cell. Bioelectrochemistry. 2024;160:108770.

https://doi.org/10.1016/j.bioelechem.2024.108770

*11*.Kadier A, Wang J, Chandrasekhar K, Abdeshahian P, Islam MA, Ghanbari F, et al. Performance optimization of microbial electrolysis cell (MEC) for palm oil mill effluent (POME) wastewater treatment and sustainable Bio-H2 production using response surface methodology (RSM). Int J Hydrogen Energy. 2022;47(34):15464-79. https://doi.org/10.1016/j.ijhydene.2021.09.259.

*12*.Arun J, SundarRajan P, Grace Pavithra K, Priyadharsini P, Shyam S, Goutham R, et al. New insights into microbial electrolysis cells (MEC) and microbial fuel cells (MFC) for simultaneous wastewater treatment and green fuel (hydrogen) generation. Fuel. 2024;355:129530. https://doi.org/10.1016/j.fuel.2023.129530

*13*.Nor MHM, Mubarak MFM, Elmi HSA, Ibrahim N, Wahab MFA, Ibrahim Z. Bioelectricity generation in microbial fuel cell using natural microflora and isolated pure culture bacteria from anaerobic palm oil mill effluent sludge. Bioresour Technol. 2015;190:458-65. https://doi.org/10.1016/j.biortech.2015.02.103.

*14*.Kadier A, Simayi Y, Abdeshahian P, Azman NF, Chandrasekhar K, Kalil MS. A comprehensive review of microbial electrolysis cells (MEC) reactor designs and configurations for sustainable hydrogen gas production. Alex Eng J. 2016;55(1):427-43. https://doi.org/10.1016/j.aej.2015.10.008.

*15*.Napoli L, Lavorante M, Franco J, Sanguinetti A, Fasoli H. Effects on nafion® 117 membrane using different strong acids in various concentrations. Journal of new materials for electrochemical systems. 2013;16(3):151-6.

*16*.Azri YM, Tou I, Sadi M. Electrodes materials evaluation in plant microbial fuel cells: a comparison of graphite and stainless steels. Biofuels. 2023;14(10):1077-86. https://doi.org/10.1080/17597269.2023.2212987.

*17*.Almatouq A, Babatunde A. Concurrent hydrogen production and phosphorus recovery in dual chamber microbial electrolysis cell. Bioresour Technol. 2017;237:193-203. https://doi.org/10.1016/j.biortech.2017.02.043.

*18*.Ziara RM, Dvorak BI, Subbiah J. Sustainable waste-to-energy technologies: Bioelectrochemical systems. Sustainable Food Waste-to-Energy Systems: Elsevier; 2018. p. 111-40. https://doi.org/10.1016/B978-0-12-811157-4.00007-3.

*19*.Wang Y, Gao Y, Hussain A, Lee H-S. Optimization of biofilm conductance measurement with two-electrode microbial electrochemical cells (MECs). Sci Total Environ. 2023;858:159577. https://doi.org/10.1016/j.scitotenv.2022.159577

*20*.Elmi H, Nor M, Ibrahim Z. Colour and COD removal from palm oil mill effluent (POME) using Pseudomonas aeruginosa strain NCIM 5223 in microbial fuel cell. J Waste Resources. 2015;5(181):2.

*21*.Bala JD, Lalung J, Al-Gheethi AAS, Kaizar H, Ismail N. Reduction of Organic Load and Biodegradation of Palm Oil Mill Effluent by Aerobic Indigenous Mixed Microbial Consortium Isolated from Palm Oil Mill Effluent (POME). Water Conservation Science and Engineering. 2018;3(3):139-56.10.1007/s41101-018-0043-9

*22*.Logan BE, Call D, Cheng S, Hamelers HV, Sleutels TH, Jeremiasse AW, et al. Microbial electrolysis cells for high yield hydrogen gas production from organic matter. Environ Sci Technol. 2008;42(23):8630-40. https://doi.org/10.1021/es801553z.

*23*.Potrykus S, León-Fernández LF, Nieznański J, Karkosiński D, Fernandez-Morales FJ. The influence of external load on the performance of microbial fuel cells. Energies. 2021;14(3):612. https://doi.org/10.3390/en14030612.

*24*.Li S, Chen G. Factors affecting the effectiveness of bioelectrochemical system applications: Data synthesis and meta-analysis. Batteries. 2018;4(3):34. https://doi.org/10.3390/batteries4030034.

*25*.Kamau J, Mbui D, Mwaniki J, Mwaura F, Kamau G. Microbial fuel cells: influence of external resistors on power, current and power density. J Thermodyn Catal. 2017;8(1):1-5.

*26*.Firdous S, Jin W, Shahid N, Bhatti Z, Iqbal A, Abbasi U, et al. The performance of microbial fuel cells treating vegetable oil industrial wastewater. Environ Technol Innov. 2018;10:143-51. https://doi.org/10.1016/j.eti.2018.02.006.

*27*.Marone A, Ayala-Campos OR, Trably E, Carmona-Martínez AA, Moscoviz R, Latrille E, et al. Coupling dark fermentation and microbial electrolysis to enhance bio-hydrogen production from agro-industrial wastewaters and by-products in a bio-refinery framework. Int J Hydrogen Energy. 2017;42(3):1609-21. https://doi.org/10.1016/j.ijhydene.2016.09.166.

*28*.Khongkliang P, Jehlee A, Kongjan P, Reungsang A, Sompong O. High efficient biohydrogen production from palm oil mill effluent by two-stage dark fermentation and microbial electrolysis under thermophilic condition. Int J Hydrogen Energy. 2019;44(60):31841-52. https://doi.org/10.1016/j.ijhydene.2019.10.022.

*29*.Fathy A, Rezk H, Yousri D, Alharbi AG, Alshammari S, Hassan YB. Maximizing Bio-Hydrogen Production from an Innovative Microbial Electrolysis Cell Using Artificial Intelligence. Sustainability. 2023;15(4):3730. https://doi.org/10.3390/su15043730.

*30*.Ndayisenga F, Yu Z, Wang B, Zhou D. Effects of the applied voltage on electroactive microbial biofilm viability and hydrogen production in a recalcitrant organic waste-fed single-chamber membrane-free microbial electrolysis cell performance. Chem Eng J. 2023;469:144002. https://doi.org/10.1016/j.cej.2023.144002.

*31*.Tan WH, Chong S, Fang H-W, Pan K-L, Mohamad M, Lim JW, et al. Microbial fuel cell technology—a critical review on scale-up issues. Processes. 2021;9(6):985. https://doi.org/10.3390/pr9060985.

*32*.Hari AR, Venkidusamy K, Katuri KP, Bagchi S, Saikaly PE. Temporal microbial community dynamics in microbial electrolysis cells–influence of acetate and propionate concentration. Front Microbiol. 2017;8:1371. https://doi.org/10.3389/fmicb.2017.01371.

*33*.Luo H, Liu G, Zhang R, Bai Y, Fu S, Hou Y. Heavy metal recovery combined with H2 production from artificial acid mine drainage using the microbial electrolysis cell. J Hazard Mater. 2014;270:153-9. https://doi.org/10.1016/j.jhazmat.2014.01.050.

*34*.Ding A, Yang Y, Sun G, Wu D. Impact of applied voltage on methane generation and microbial activities in an anaerobic microbial electrolysis cell (MEC). Chem Eng J. 2016;283:260-5. https://doi.org/10.1016/j.cej.2015.07.054

*35*.Kadier A, Kalil MS, Abdeshahian P, Chandrasekhar K, Mohamed A, Azman NF, et al. Recent advances and emerging challenges in microbial electrolysis cells (MECs) for microbial production of hydrogen and value-added chemicals. Renew Sust Energ Rev. 2016;61:501-25. https://doi.org/10.1016/j.rser.2016.04.017

*36*.Mejía-López M, Verea L, Verde A, Lara B, Campos J, Najera M, et al. Improvement of the carbon electrode treatment to obtain bioanodes for microbial electrolysis cell (MEC). Int J Electrochem Sci. 2018;13(4):3970-85. https://doi.org/10.20964/2018.04.64.

*37*.Wang A, Liu W, Ren N, Zhou J, Cheng S. Key factors affecting microbial anode potential in a microbial electrolysis cell for H2 production. Int J Hydrogen Energy. 2010;35(24):13481-7. https://doi.org/10.1016/j.ijhydene.2009.11.125.

*38*.Liu W-z, Wang A-j, Ren N-q, Zhao X-y, Liu L-h, Yu Z-g, et al. Electrochemically assisted biohydrogen production from acetate. Energy & fuels. 2008;22(1):159-63. https://doi.org/10.1021/ef700293e.

*39*.Logan BE. Energy diversity brings stability. Environmental Science and Technology. 2006;40(17):5161.

*40*.Chonde A. Microbial fuel cell: a new approach of wastewater treatment with power generation. International Journal of Chemical, Environmental and Pharmaceutical Research. 2014;5(1):8-12.

*41*.Zain SM, Roslani NS, Hashim R, Anuar N, Suja F, Wan Daud W, et al. Microbial Fuel Cells using Mixed Cultures of Wastewater for Electricity Generation. Sains Malaysiana. 2011;40:993-7.

*42*.Ghangrekar M, Shinde V, editors. Microbial fuel cell: a new approach of wastewater treatment with power generation. International Workshop on R&D Frontiers in Water and Wastewater Management Nagpur, India; 2006: Citeseer.

*43*.Fischer F, Sugnaux M, Savy C, Hugenin G. Microbial fuel cell stack power to lithium battery stack: pilot concept for scale up. Appl Energy. 2018;230:1633-44. https://doi.org/10.1016/j.apenergy.2018.09.030.

*44*.Obileke K, Onyeaka H, Meyer EL, Nwokolo N. Microbial fuel cells, a renewable energy technology for bio-electricity generation: A mini-review. Electrochem Commun. 2021;125:107003. https://doi.org/10.1016/j.elecom.2021.107003.

*45*.Daud SM, Daud WRW, Bakar MHA, Kim BH, Somalu MR, Muchtar A, et al. Low-cost novel clay earthenware as separator in microbial electrochemical technology for power output improvement. Bioprocess and biosystems engineering. 2020;43:1369-79. https://doi.org/10.1007/s00449-020-02331-7.

*46*.Yang W, Li J, Fu Q, Zhang L, Wei Z, Liao Q, et al. Minimizing mass transfer losses in microbial fuel cells: theories, progresses and prospectives. Renew Sust Energ Rev. 2021;136:110460. https://doi.org/10.1016/j.rser.2020.110460.

*47*.Kloch M, Toczyłowska-Mamińska R. Toward optimization of wood industry wastewater treatment in microbial fuel cells—Mixed wastewaters approach. Energies. 2020;13(1):263. https://doi.org/10.3390/en13010263.

*48*.Miran W, Nawaz M, Jang J, Lee DS. Sustainable electricity generation by biodegradation of low-cost lemon peel biomass in a dual chamber microbial fuel cell. International Biodeterioration & Biodegradation. 2016;106:75-9. https://doi.org/10.1016/j.ibiod.2015.10.009.

*49*.Wang D, Wang Y, Yang J, He X, Wang R-J, Lu Z-S, et al. Cellulose aerogel derived hierarchical porous carbon for enhancing flavin-based interfacial electron transfer in microbial fuel cells. Polymers. 2020;12(3):664. https://doi.org/10.3390/polym12030664.

*50*.Rabaey K, Boon N, Siciliano SD, Verhaege M, Verstraete W. Biofuel cells select for microbial consortia that self-mediate electron transfer. Appli and env microbio. 2004;70(9):5373-82. https://doi.org/10.1128/AEM.70.9.5373-5382.2004.

Table 1. Preliminary results obtained from MEC

| Parameters | | MEC Batch | | | | | | | | | |
|---|---|---|---|---|---|---|---|---|---|---|---|
| | | 1 | 2 | 3 | 4 | 5 | 6 | 7 | 8 | 9 | 10 |
| COD (mg/L) | Initial | 150 | 206 | 315 | 770 | 790 | 915 | 980 | 1635 | 1855 | 1930 |
| | Final | 138 | 95 | 185 | 635 | 625 | 1085 | 815 | 1560 | 1905 | 1920 |
| | Removal Efficiency (%) | 8 | 53.88 | 41.27 | 17.53 | 20.89 | N/A | 16.84 | 4.59 | N/A | 0.52 |
| | COD removed | 12 | 111 | 130 | 135 | 165 | N/A | 165 | 75 | N/A | 10 |
| Average voltage supplied (V) | | 1.198 | 0.679 | 0.199 | 0.176 | 1.343 | 1.104 | 1.198 | 0.758 | 0.661 | 1.187 |
| Average voltage across the resistor (mV) | | 5.75 | 1 | 0.1 | 0.2 | 2.25 | 22.5 | 5.75 | 1 | 9.5 | 2 |
| Average voltage applied (V) | | 1.192 | 0.678 | 0.199 | 0.176 | 1.341 | 1.081 | 1.192 | 0.757 | 0.652 | 1.185 |
| Current (mA) | | 0.575 | 0.1 | 0.01 | 0.02 | 0.255 | 2.25 | 0.575 | 0.1 | 0.95 | 0.2 |
| Current Density (mA/m$^2$) | | 152.12 | 26.46 | 2.65 | 5.29 | 59.52 | 595.24 | 152.12 | 26.46 | 251.32 | 52.91 |
| Cumulative Hydrogen Production (mL) | | 37.8 | 0.6 | 104.4 | 92.4 | 17.4 | 69.6 | 37.8 | 33 | 93 | 37.8 |
| Hydrogen production rate (mL/day) | | 12.6 | 0.2 | 34.8 | 30.8 | 5.8 | 23.2 | 12.6 | 11 | 31 | 12.6 |

| | | | | | | | | | | | |
|---|---|---|---|---|---|---|---|---|---|---|---|
| Hydrogen production per COD removed ($m^3$ $H_2$/kg COD removed) | | N/A | 0.167 | 3.135 | 2.369 | 0.43 | 1.406 | N/A | 0.667 | 4.133 | N/A |
| Coulombic Efficiency (%) | | N/A | 59.7 | 0.65 | 1.1 | 11.94 | 97.69 | N/A | 4.34 | 0.91 | N/A |
| pH | Anode final | 6.74 | 6.92 | 6.68 | 6.44 | 6.2 | 6.76 | 6.77 | 6.14 | 6.29 | 6.26 |
| | Cathode final | 6.98 | 6.98 | 7.01 | 7.02 | 7.01 | 7.27 | 7.32 | 7.01 | 7.18 | 7.15 |
| | Difference | 0.24 | 0.06 | 0.33 | 0.58 | 0.81 | 0.51 | 0.55 | 0.87 | 0.89 | 0.89 |

Table 2. Experimental condition and results input for CCD

| Run | Parameter | | Response | | |
|---|---|---|---|---|---|
| | A: Influent COD Level (mg/l) | B: Voltage Supply (V) | Cumulative Hydrogen Production (mL) | Hydrogen Production Rate (mL/day) | COD Removal Efficiency (%) |
| 1 | 980 | 0.758 | 33.0 | 11.0 | 16.84 |
| 2 | 1930 | 0.170 | 67.8 | 22.6 | 0.52 |
| 3 | 315 | 0.176 | 92.4 | 30.8 | 41.27 |
| 4 | 206 | 0.199 | 104.4 | 34.8 | 53.88 |
| 5 | 770 | 1.343 | 17.4 | 5.8 | 17.53 |
| 6 | 980 | 0.758 | 33.0 | 11.0 | 16.84 |
| 7 | 315 | 0.176 | 92.4 | 30.8 | 41.27 |
| 8 | 206 | 0.199 | 104.4 | 34.8 | 53.88 |
| 9 | 770 | 1.343 | 17.4 | 5.8 | 17.53 |

Table 3. Results obtained from MFC

| Parameters | MFC Batch | | | | |
|---|---|---|---|---|---|
| | 1 | 2 | 3 | 4 | 5 |
| Average voltage across the resistor (mV) | 14 | 60 | 195 | 291 | 338 |
| Voltage on day 4 (mV) | 10 | 117 | 201 | 268 | 327 |
| Current (mA) | 0.0100 | 0.0355 | 0.0394 | 0.0268 | 0.0076 |
| Power (μW) | 0.1000 | 4.1482 | 7.9218 | 7.1824 | 2.4867 |
| Current density (mA/m$^2$) | 2.65 | 9.38 | 10.43 | 7.09 | 2.01 |
| Power density (μW/m$^2$) | 26.46 | 1097.40 | 2095.70 | 1900.11 | 657.86 |
| Resistance of the resistor (Ω) | 1000 | 3300 | 5100 | 10000 | 43000 |
| Coulombic Efficiency (%) | 0.036 | 0.231 | 0.076 | 0.074 | N/A |
| COD Removal Efficiency (%) | 22.47 | 31.58 | 62.71 | 68.42 | 64.85 |
| pH Anode final | 7.13 | 7.31 | 7.29 | 7.39 | 7.41 |

| | | | | | |
|---|---|---|---|---|---|
| Cathode final | 7.41 | 7.51 | 7.51 | 7.51 | 7.47 |
| Difference | 0.28 | 0.20 | 0.22 | 0.12 | 0.06 |

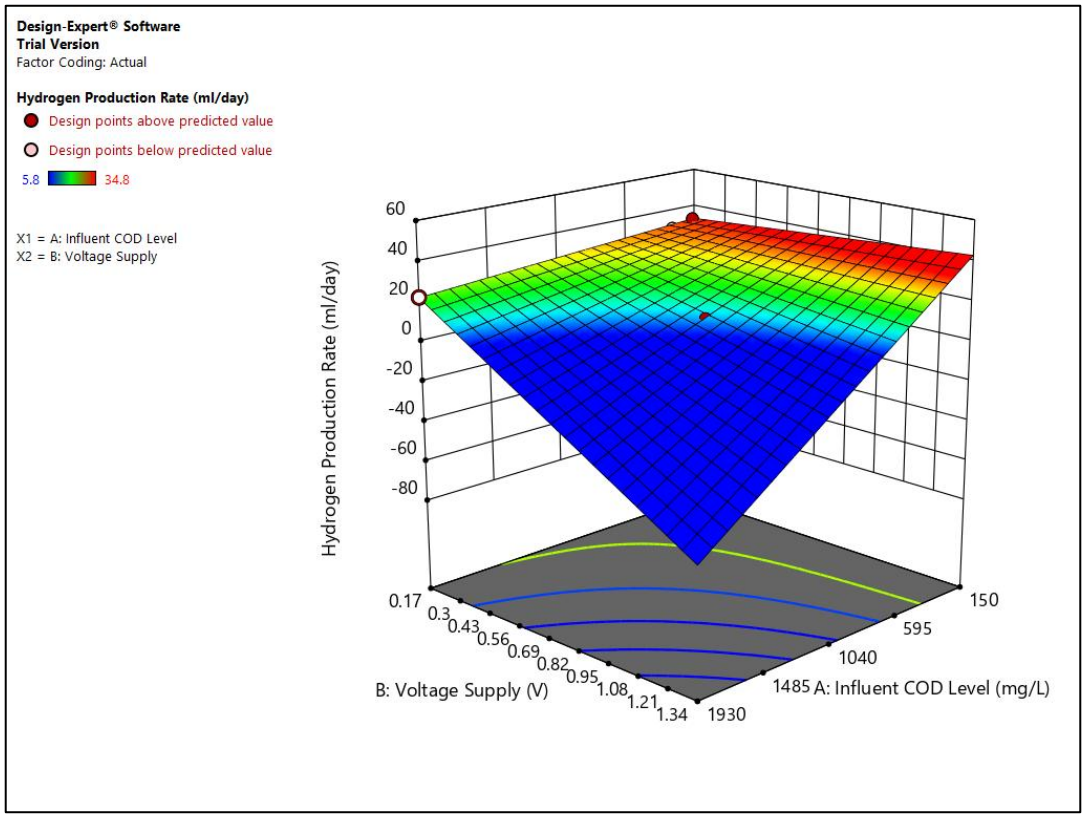


Fig. 1. Response surface of hydrogen production rate as a function of influent COD level and applied voltage.

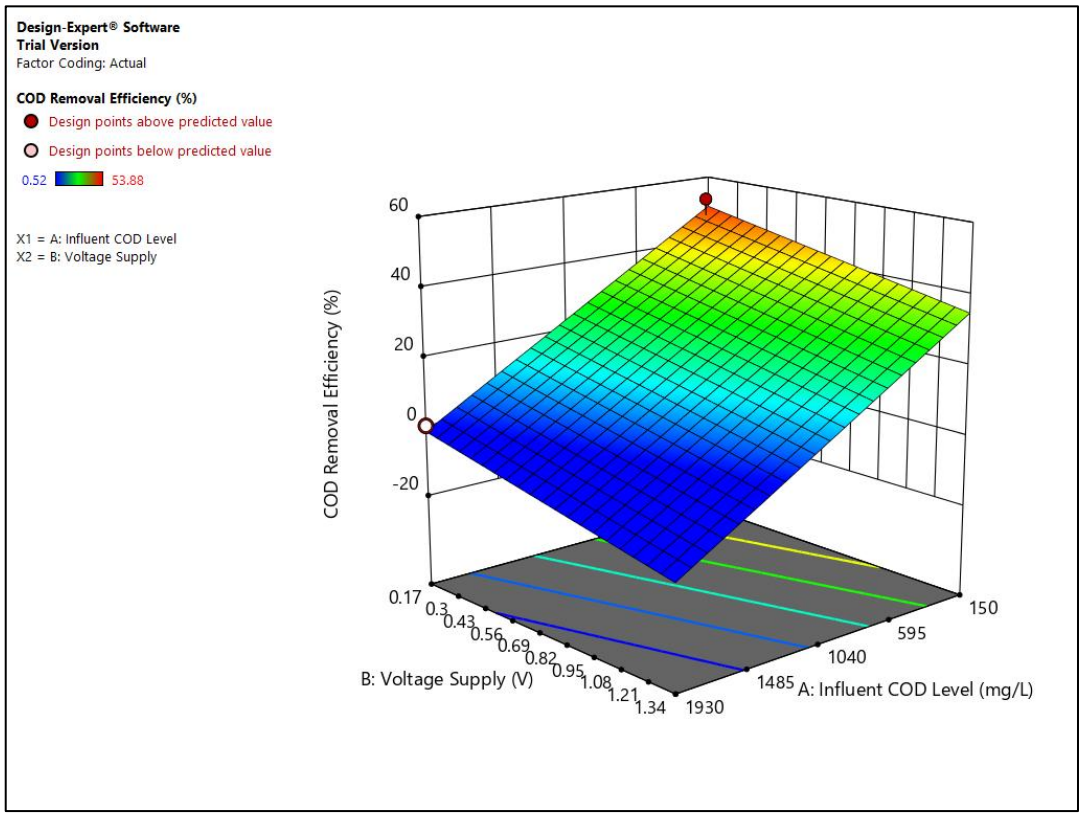


Fig. 2. Response surface of COD removal efficiency as a function of influent COD level and applied voltage.

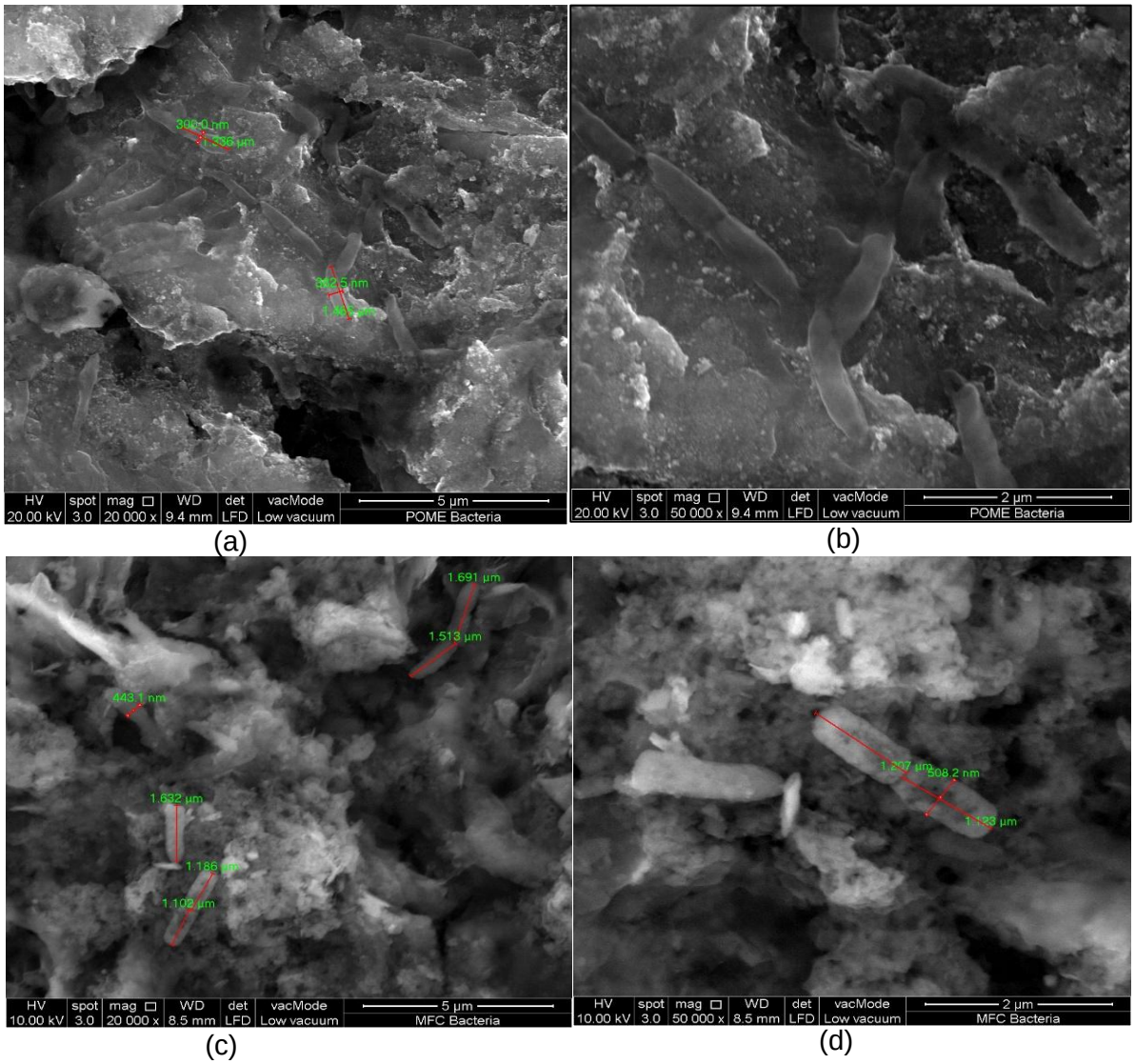


Fig. 3. Bacteria found on the anode electrode of MEC at a) 20,000x b) 50,000x magnification. Bacteria found on the anode electrode of MFC at c) 20,000x d) 50,000x magnification.

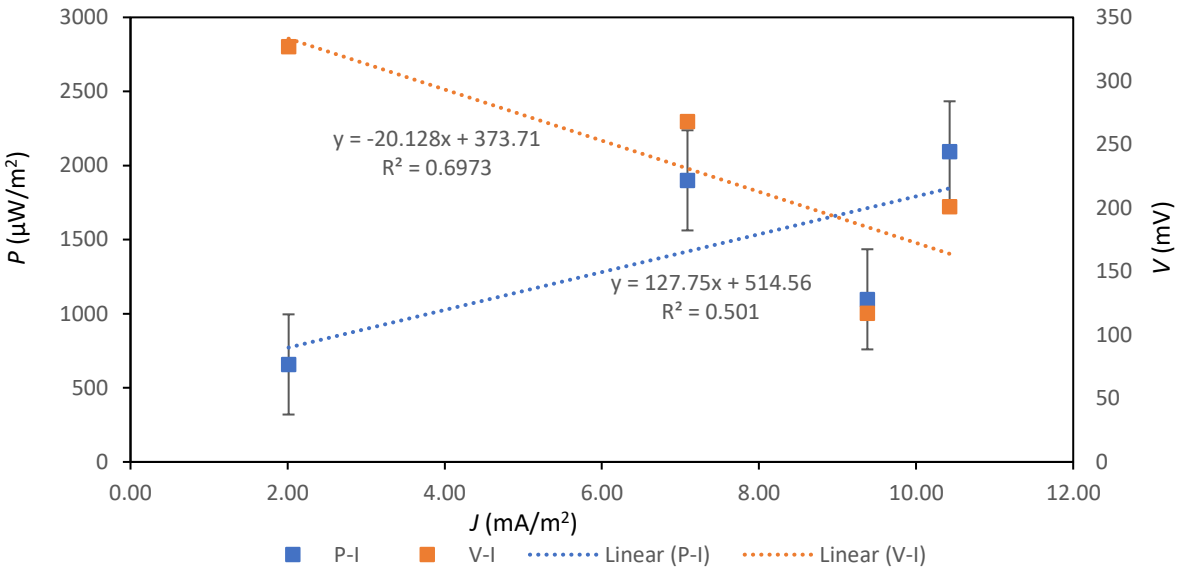


Fig. 4. Polarisation and power density curves.

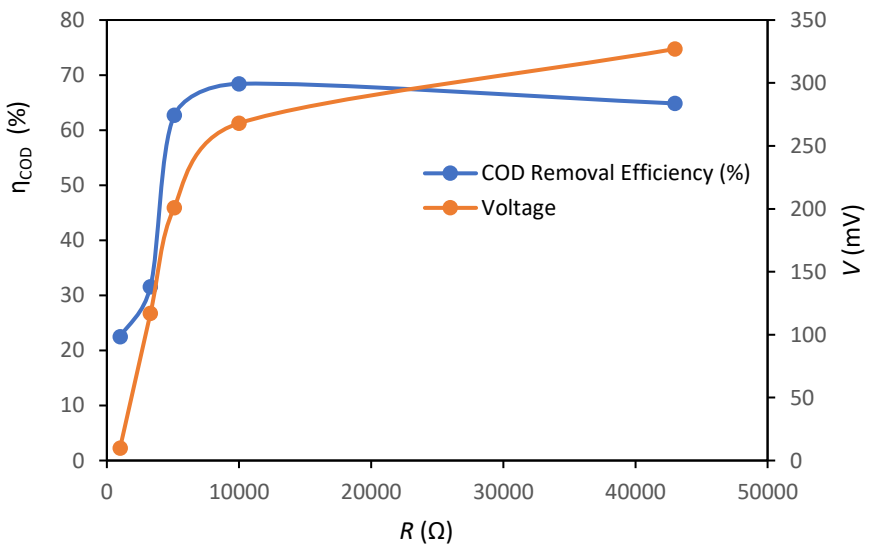


Fig. 5. Graph of COD removal efficiency and voltage produced against resistance.

## Supplementary materials

Table S1. ANOVA for the model of hydrogen production rate and COD removal efficiency.

| Source | Sum of Squares | DF | Mean Square | F-Value | P-Value |
|---|---|---|---|---|---|
| Hydrogen Production Rate (2FI model) | | | | | |
| Model | 1227.14 | 3 | 409.05 | 201.00 | < 0.0001 |
| A-COD Level | 75.17 | 1 | 75.17 | 36.93 | 0.0017 |
| B-Voltage Supply | 327.02 | 1 | 327.02 | 160.69 | < 0.0001 |
| AB | 45.90 | 1 | 45.90 | 22.55 | 0.0051 |
| Residual | 10.18 | 5 | 2.04 | | |
| Lack of Fit | 10.18 | 1 | 10.18 | | |
| Pure Error | 0.0000 | 4 | 0.0000 | | |
| Total | 1237.32 | 8 | | | |
| | | | | | |
| COD removal efficiency (Linear Model) | | | | | |
| Model | 2803.80 | 2 | 1401.90 | 80.05 | < 0.0001 |
| A-COD Level | 2046.02 | 1 | 2046.02 | 116.84 | < 0.0001 |
| B-Voltage Supply | 366.26 | 1 | 366.26 | 20.92 | 0.0038 |
| Residual | 105.07 | 6 | 17.51 | | |
| Lack of Fit | 105.07 | 2 | 52.54 | | |
| Pure Error | 0.0000 | 4 | 0.0000 | | |
| Total | 2908.87 | 8 | | | |

Table S2. MEC optimised value from Design expert software

| No. | Influent COD Level (mg/L) | Voltage Supply (V) | Hydrogen Production Rate (mL/day) | COD Removal Efficiency (%) | Desirability |
|---|---|---|---|---|---|
| 1 | 150.001 | 0.338 | 34.800 | 48.680 | 0.966 |
| 2 | 150.001 | 0.304 | 34.532 | 49.142 | 0.963 |
| 3 | 150.000 | 0.274 | 34.290 | 49.557 | 0.961 |

| | | | | | |
|---|---|---|---|---|---|
| 4 | 150.001 | 0.229 | 33.931 | 50.176 | 0.957 |
| 5 | 150.000 | 0.222 | 33.875 | 50.272 | 0.956 |
| 6 | 150.005 | 0.193 | 33.646 | 50.666 | 0.953 |
| 7 | 150.002 | 0.189 | 33.611 | 50.725 | 0.953 |
| 8 | 150.001 | 0.596 | 36.855 | 45.146 | 0.942 |
| 9 | 150.001 | 0.681 | 37.535 | 43.975 | 0.934 |
| 10 | 150.004 | 0.863 | 38.984 | 41.482 | 0.916 |
| 11 | 150.003 | 0.895 | 39.240 | 41.042 | 0.912 |

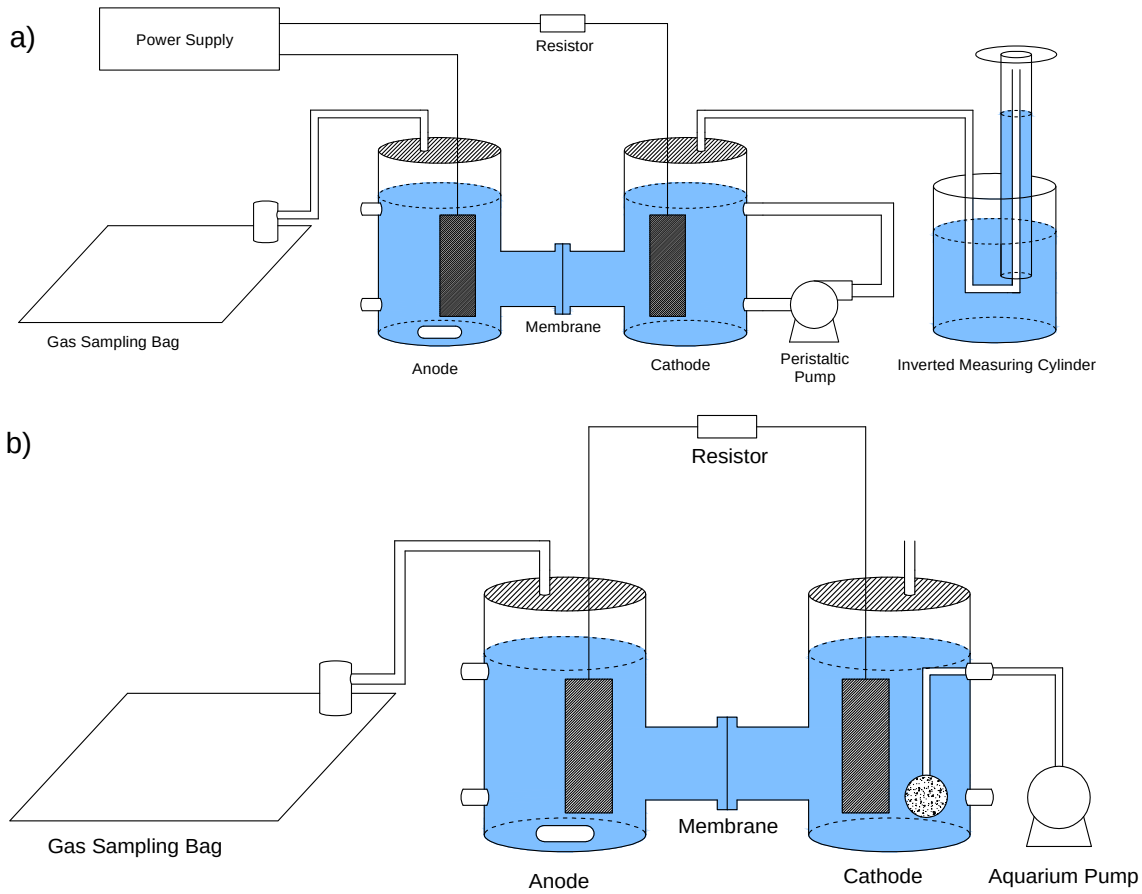


Fig. S1. Schematic diagram of a) MEC and b) MFC

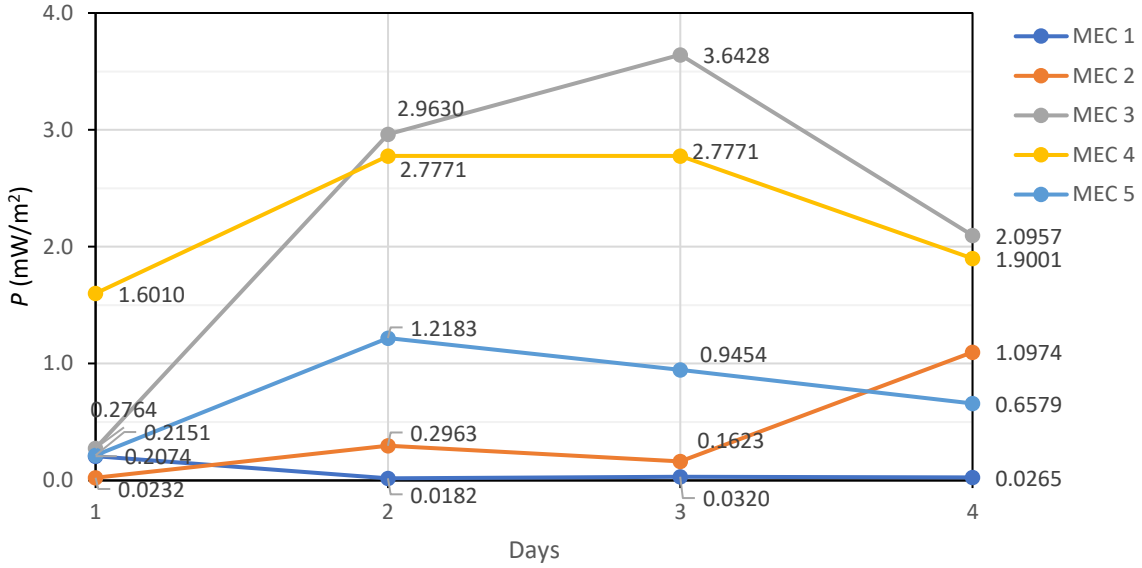


Fig. S2. Daily power generation of MFC